Ultrafast spin crossover photochemical mechanism in $[Fe^{II}(2,2'-bipyridine)_3]^{2+}$ revealed by quantum dynamics

Swarnendu Bhattacharyya,[a] Marc Alías-Rodríguez,[a] and Miquel Huix-Rotllant[b]
Aix-Marseille Univ, CNRS, ICR, Marseille, France.

The photoinduced spin crossover reaction of $[Fe^{II}(2,2'-bipyridine)_3]^{2+}$ is a light-induced transformation of the initial singlet low-spin configuration ($^1A_1$) in a quintet high-spin state ($^5T_2$) in the sub-picosecond timescale. The photochemical mechanism is still under debate, especially concerning the role of triplet intermediate excited states. Using wavepacket dynamics, we show that, upon excitation to a metal-ligand charge transfer (MLCT) state, the metal-centered (MC) triplet manifold ($^3T_1$) is responsible for the ultrafast transfer to the $^5T_2$ state, leading to a mechanism of the type ^{1}MLCT$\rightarrow$ ^{3}MLCT $\rightarrow$ $^3T_1 \rightarrow$ $^5T_2$. This photochemical pathway is possible thanks to the ligand vibronic effects on increasing the effective triplet/quintet metal-centered couplings, facilitating the relaxation in the MLCT band and modulating the relative position of the MC states to allow an efficient transfer population between MLCT and MC.

Molecules and materials containing d^4 to d^7 octahedral metal complexes exhibit a magnetic bistability known as spin crossover (SCO). Such materials have wide range of applications such as thermochromic paints, molecular electronics, nanophotonic devices and mechanical actuators, to mention just a few.[1–5] Essentially, the SCO reaction consists in a transition from a low-spin (LS) to a high-spin (HS) electronic configuration. The SCO can be stimulated by several kinds of external perturbations such as pressure,[6] temperature,[7] electromagnetic radiation,[8–13] etc. The mechanisms of light-induced SCO (LISCO) are perhaps the least understood, despite the numerous experimental and theoretical studies.[14–19] On the one hand, the interpretation of time-resolved spectroscopy is frequently hampered by the complexity of the electronic structure and the ultrafast nature of the LISCO reactions (usually happening in a few tens of femtoseconds), requiring thus the back up of theoretical simulations for helping out in the resolution of mechanisms.[20] On the other hand, theoretical models require a balanced treatment of strong electron-vibrational and spin-orbit couplings of electronic excited state bands of several spin multiplicities, that require state-of-the-art methodologies both in electronic structure and quantum dynamics.[21]

Here, we develop a theoretical model for describing the LISCO mechanism of a well-known iron complex, $[Fe(bpy)_3]^{2+}$ (bpy=2,2'-bipyridine) (see Fig. S1). This complex has been perhaps one of the best studied in the literature, although there exist discrepancies on the photochemical mechanism.[8–19] It is commonly accepted that the low-spin (LS) state of $[Fe(bpy)_3]^{2+}$ corresponds to a singlet closed-shell configuration ($^1A_1$), in which six nitrogens form a dative covalent bond with the iron center. Note that the electronic states on iron are labelled according to O_h point group as it is customary in the literature, despite the complex has a lower D_3 symmetry in its ground state. The high-spin (HS) states are constituted by a quintet triad ($^5T_2$) with a gap of ca. 0.1 eV due to a small Jahn-Teller distortion of the HS states.[22] Compared to the LS minimum energy geometry, the HS is characterized by a symmetric increase of the Fe-N distances (+0.2 Å) and a slight decrease (-5.7°) of the N-Fe-N bite angle. This is a consequence of the occupation of e_g orbitals with Fe-N σ^* antibonding character. $[Fe(bpy)_3]^{2+}$ is a low-spin complex and does not exhibit thermal SCO at room temperature due to the large HS-LS energy gap, in agreement with the difference of 5565 cm^{-1} reported theoretically by Sousa et al.,[16] explaining the $^5T_2$ state short lifetime (650 ps).[23,24] $[Fe(bpy)_3]^{2+}$ exhibits a maximum absorbance at 520 nm in the visible part absorption spectrum, which corresponds to a metal-to-ligand-charge-transfer (MLCT) state and another peak at 350 nm corresponding to a different set of MLCT states.[25] The complex excited state band structure has been challenging for theoretical simulations of the UV-visible absorption spectrum, showing a strong influence on the geometry distortions of the complex in solution.[14,15,26]

The photochemical LISCO mechanism in $[Fe(bpy)_3]^{2+}$ is still unclear. One of the first studies, by McCusker et al. suggested a direct ^{1}MLCT$\rightarrow$$^5T_2$ transition in less than 700 fs according to UV-visible transient absorption spectroscopy.[27] The main confusion comes from the involved excited state intermediates. Auböck et al. based on high-resolution (<40 fs) UV-visible pump-probe spectroscopy determined a "direct" mechanism, ^{1}MLCT $\rightarrow$ ^{3} MLCT $\rightarrow$ $^5T_2$ assisted by high-frequency ligand modes.[12] Lemke et al. confirmed the "direct" mechanism using time-resolved X-ray Absorption Spectroscopy at sub-30-fs resolution, estimating the transfer rate to 120 fs, and a coherent vibration of 265 fs period corresponding to Fe-N_6 breathing.[13] In contract, an "indirect" mechanism ^{1}MLCT$\rightarrow$ ^{3}MLCT$\rightarrow$ ^{3}MC$\rightarrow$HS was pointed out by Gawelda et al. based on fluorescence and transient absorption spectroscopy, from which kinetic rates of 15 fs for singlet/triplet transfer, 120 fs for ^{3}MLCT$\rightarrow$ ^{3}MC states and 960 fs for the triplet/quintet transfer.[8] Similar conclusions were reached by Zhang et al. using time-resolved X-ray K_β fluorescence spectroscopy.[11] Fi-

[a] These two authors contributed equally
[b] Electronic mail: miquel.huix-rotllant@cnrs.fr

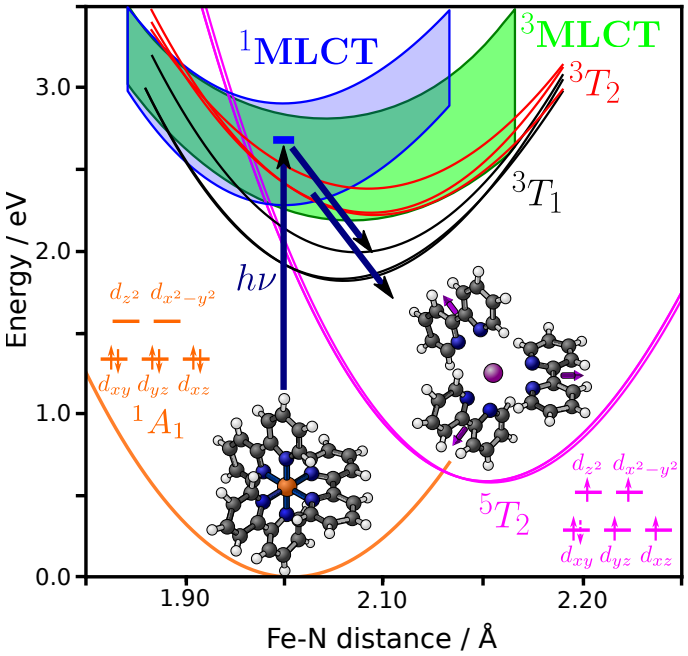

FIG. S1: Schematic representation of the potential energy surfaces and geometric changes induced by light absorption from the low-spin (^{1}A$_1$) to high-spin (^{5}T$_2$) transition in $[Fe(bpy)_3]^{2+}$.

nally, Moguilevski et al. using ultrafast XUV photoemission spectroscopy determined that both "direct' and "indirect" mechanisms are in competition, but the indirect dominates the process.[28] From a theoretical perspective, Sousa et al. computed the ISC kinetic rates using Fermi's golden rule, determining a dominant indirect mechanism.[16] Taking into account thermal disorder, the "direct" mechanism was later on estimated possible, due to a mixing between MC and MLCT states that leads to stronger spin-orbit couplings of the ^{3}MLCT and the HS state.[17] The wavepacket quantum dynamics methodology were employed by Penfold and coworkers to explain Fe(II) high-efficient photosensitizers because of the large ^{3}MLCT lifetime of the complexes with N-heterocyclic carbene ligands compared with the prototypical $Fe(bpy)_3$ complex.[29] For $Fe(NHC)_6$, Pápai determined the LISCO mechanism via wavepacket dynamics and trajectory surface hopping for another Fe(II) octahedral complex, showing a 100 fs transfer from the ^{1}T$_{1g}$ states to the ^{3}T$_{2g}$ followed by a branching towards the ^{1}A$_{1g}$, ^{5}T$_{2g}$ and ^{3}T$_{1g}$ activated through the Fe-N asymmetric stretching Jahn-Teller modes.[30,31]

Here, we construct a vibronic model Hamiltonian for describing the LISCO reaction in $[Fe(bpy)_3]^{2+}$ containing 13 singlets, 15 triplets and 3 quintets (see Fig. S1). The lowest part of the excited state spectrum can be characterized either by a d-d type transitions (i.e., the MC states) or a d- to π_1^* orbitals on the bipyridine units (MLCT). The π_1^* corresponds to a C_2-$C_{2'}$ π-type orbital and a N-C_2/N-$C_{2'}$ π^*-type, which is common of diimine bonds (in the supporting information, see Fig. S1 for the numeration of bipyridine atoms, and Fig. S2 for the molecular orbital shape). The π^* orbitals have an $a_2 \oplus e$ symmetry and are delocalized over the three equivalent bipyridine units. The singlet bright states are found in the middle of the MLCT band and have $t_{2g} \rightarrow \pi_1^*$ character. The excitation at the ^{1}A$_1$ minimum is 2.65 eV, with oscillator strength of $8.5{\cdot}10^{-2}$ a.u. The rest of the singlet MLCT band is dark, and it is found in energies ranging from 2.28 to 2.90 eV. The ^{1}T$_1$ lie at the upper end of the MLCT band (around 3 eV) and thus not accessible in the lower range of the absorption spectrum, but have also been included in the model. The triplet manifold also consists of an MLCT band found between 2.09-2.51 eV, overlapping with the singlet MLCT band, as well as the ^{3}MC and the ^{5}T$_2$. The ^{3}T$_1$ is found in a range of 1.91-2.13 eVs (overlapping with the lower part of the $^{1/3}$MLCT bands), while the ^{3}T$_2$ lies between 2.41-2.62 eV (overlapping with the upper part of the $^{1/3}$MLCT bands).

The excited state energies are computed along 9 vibrational modes described in terms of normal modes coordinates (see more details in the Supporting Information). The main mode is the reaction coordinate (depicted in Fig. S1), defined as the normal mode expansion of the mass-weighted HS-LS geometric difference. This consists essentially of a symmetric stretching of the center of mass of the three bipyridine moieties. Two other Fe-N modes are included, consisting of Jahn-Teller asymmetric stretching modes that distort the complex in axial/equatorial planes. The remaining modes are on the ligands, corresponding to a C_2-$C_{2'}$ and C_2-N/$C_{2'}$-N stretching modes of the bipyridine rings, formed by two sets of Jahn-Teller distortions and two "tuning modes", that is, modes that modulate the energetic gaps between states and account essentially for the relaxation in the MLCT bands.

The vibronic model has been used in a quantum dynamics simulation starting from a wavepacket corresponding to an equal population of the bright ^{1}MLCT states. The results for the first 0.5 ps are shown in Fig. S2. As it can be observed, the population on the ^{1}MLCT rapidly decays and becomes negligible after 150 fs. The first decay of the ^{1}MLCT is concomitant to rapid grow of the ^{3}MLCT population, which becomes dominant at around 50 fs. Afterwards, the ^{3}MLCT population decays rapidly. The wavepacket is then split into three different populations. The dynamic evolution of populations of the two ^{3}MC states behaves similarly. On the one hand, the ^{3}T$_1$, which receives 30% of the population, exhibits a rapid grow from the beginning slow decay after 150 fs. On the other hand, the ^{3}T$_2$, which receives 10% of the population has a slow decay after 100 fs. The quintet ^{5}T$_2$ has a rapid and steady grow starting at around 50 fs until the end of the dynamics, becoming the dominant population after around 120 fs.

The main unresolved question about the LISCO mechanism is the role of excited state intermediates that

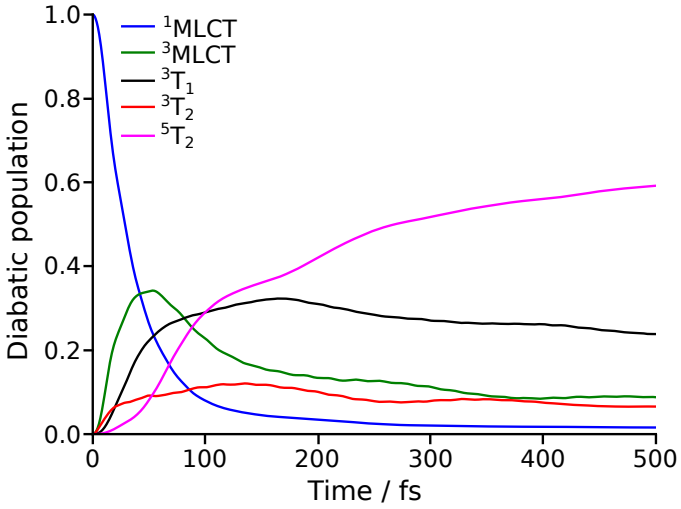

FIG. S2: (top) Evolution of diabatic populations of the singlet and triplet MLCTs, triplet MCs and $^5T_2$ states during the first 0.5 ps.

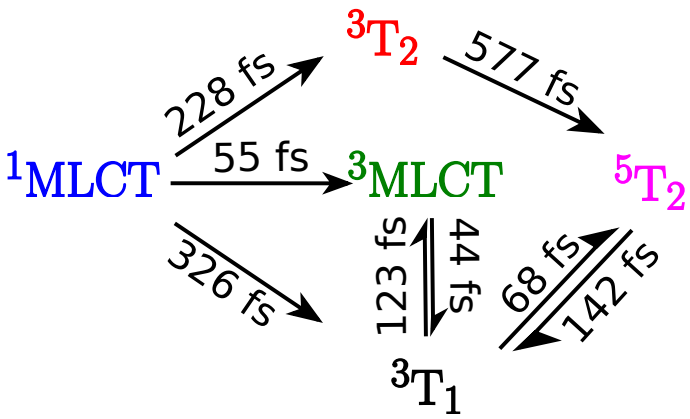

FIG. S3: First-order kinetic model extracted from the fitting of kinetic rates from the wavepacket dynamics simulations shown in Fig. S2.

leads to the HS state, either via a "direct mechanism" (^{3}MLCT→ HS) or an "indirect mechanism" (^{3}MC→ HS). To extract the mechanism from the evolution of diabatic population, we performed wavepacket dynamics on reduced models, in which we deactivate certain interstate couplings or vibrations (see further details in Sec. S3D of the supporting information). This allows to infer the allowed pathways in the excited state that lead to the evolution of the total diabatic populations.

We do not observe a major transfer to the HS state when deactivating the ^{3}MLCT couplings with the ^{3}MC, clearly evidencing a "indirect" mechanism. This is in agreement with the weak spin-orbit coupling between^{3}MLCT and $^5T_2$. Still, when triplet MLCT/MC are absent, some HS state is build up due to the ^{1}MLCT→$^3T_1/^3T_2$. The deactivation of the ^{3}MLCT/HS coupling shows the same results as the full model (see Fig. S14 in the supporting information), thus excluding the possibility of a "direct" mechanism. On the other hand, deactivating ^{3}MC/HS does not lead to HS population transfer (see Fig. S16 in the supporting information), indicating that the MC states are the intermediates responsible for the population of HS state. Finally, the deactivation of the $^3T_2$/HS does not exhibit significant differences in the HS population. Therefore, the $^3T_1$ is the main intermediate populating the $^5T_2$ state.

From these quantum dynamics results, one can infer a global first-order kinetic model for the LISCO reaction of $[Fe(bpy)_3]^{2+}$. To obtain the rates for each process, the kinetic rates have been optimized to fit the evolution of diabatic populations obtained by the wavepacket dynamics with the full model (for further details, see Sec. S3B in the supporting information). The results are summarized in the scheme in Fig. S3. On the one hand, the total singlet/triplet transfer transfer takes 40 fs (see Fig. S10 in the supporting information), slightly slower than the <30 fs transfer observed experimentally.[10] This transfer can be decomposed in a fast transfer to the triplet MLCT, which takes 55 fs, and two slower transfers directly to the $^3T_1$ and $^3T_2$ MC states in 326 fs and 228 fs, respectively. The total triplet/quintet transfer takes place in 178 fs (see Fig. S10 in the supporting information), in good agremement with the 120-130 fs reported in the literature 8–11,13. The role of the triplet intermediates is now clarified in Fig. S3. An equilibrium is established in the triplet MLCT/MC, ^{3}MLCT ↔ $^3T_1$ with a forward and backward kinetic rate of 44 and 123 fs respectively, thus favoring the population of $^3T_1$. The HS state is populated via a fast decay from the $^3T_1$ state (68 fs), and a slower decay from the $^3T_2$ state (577 fs). A back transfer reaction from the HS to the $^3T_1$ states is possible, with a transfer rate of 142 fs. This back transfer reaction is related to the ISC in the reverse-SCO from the vibrationally hot $^5T_2$ state some of us proposed in related Fe(II) complexes.[19]

The role of the different vibrational modes in the ultrafast mechanism has been also a matter of discussion.[12,13] Previous studies agree that the symmetric Fe-N stretching is the dominant mode activated during the LISCO photoprocess. We confirm this observation from wavepacket dynamics, in which the Fe-N distance is increased by ca. 0.10 Å during the dynamics (see Fig. S11 in the supporting information). This evolution is explained by the fact that ^{3}MC and the HS states are populated, in which e_g orbitals are occupied which are σ^* type orbitals for the Fe-N distance. Axial and equatorial Fe-N distance evolve similarly, indicating an absence of strong excited state Jahn-Teller distortions are observed in this complex. The N-Fe-N bite angle (see Fig. S12 in the supporting information) slightly increases ($\approx 0.5°$) during the first 20 fs of the simulation, because of the initial population of the MLCT states that induce a charge transfer to the bipyridines. After the transfer to the ^{3}MC and HS states, the angle decreases steadily to reach a value around -3.0° than the ground state equilibrium ge-

ometry. The C-C bond (see Fig. S13 in the supporting information) initially decreases because of the population of the MLCT states which stabilize at a shorter distances because of the π bonding character within the so-called π_1^* orbital. Thereafter, the C_2-$C_{2'}$ distance increases as a consequence of the enlarged Fe-N distance. As stated by Auböck et al.[12], the high-frequency modes in bipyridine play a key role in the process. These modes allow an efficient ISC and a relaxation in the MLCT band. The exclusion of these modes in a reduced model dynamics does not allow an effective transfer from the ^{1}MLCT manifold and the population remain trapped in these states (see Fig. S20 in the supporting information).

In conclusion, the apparent discrepancy between the mechanisms in $[Fe(bpy)_3]^{2+}$ is clarified through the use of quantum dynamics. These simulations indicate that the ^{3}MC states are necessary intermediates to populate the HS state ("indirect" mechanism). The "direct" mechanism from the ^{3}MLCT manifold is negligible. The ultrafast LISCO reaction is essentially explained by the interplay between the energetic proximity of MLCT and MC bands, as well as fast C_2-$C_{2'}$ stretching of the ligands that allows a strong electron-vibrational couplings, without the need of strong Jahn-Teller type distortions. These results clarify the LISCO mechanism of $[Fe(bpy)_3]^{2+}$ and points out the important role of the ligands in modulating the reaction mechanism.

ACKNOWLEDGEMENTS

We acknowledge financial support by the "Agence Nationale pour la Recherche" through the project MULTICROSS (ANR-19-CE29-0018). Centre de Calcul Intensif d'Aix-Marseille is acknowledged for granting access to its high performance computing resources.

CONFLICT OF INTEREST

Please enter any conflict of interest to declare.

[1] J.-F. Létard, P. Guionneau, L. Goux-Capes, Towards Spin Crossover Applications, pages 221–249, Springer Berlin Heidelberg, Berlin, Heidelberg **2004**.
[2] M. A. Halcrow (Editor), Spin-crossover materials, John Wiley & Sons, Nashville, TN **2013**.
[3] G. Molnár, L. Salmon, W. Nicolazzi, F. Terki, A. Bousseksou, J. Mater. Chem. C **2014**, 2, 1360.
[4] A. Enriquez-Cabrera, A. Rapakousiou, M. Piedrahita Bello, G. Molnár, L. Salmon, A. Bousseksou, Coordination Chemistry Reviews **2020**, page 213396.
[5] S. Rat, M. Piedrahita-Bello, L. Salmon, G. Molnár, P. Demont, A. Bousseksou, Advanced Materials **2018**, 30, 1705275.
[6] I. Rusu, I. C. Manolache-Rusu, A. Diaconu, O. Palamarciuc, I. A. Gural'skiy, G. Molnar, A. Rotaru, Journal of Applied Physics **2021**, 129, 064501.
[7] V. M. Hiiuk, S. Shova, A. Rotaru, V. Ksenofontov, I. O. Fritsky, I. A. Gural'skiy, Chem. Commun. **2019**, 55, 3359.
[8] W. Gawelda, A. Cannizzo, V.-T. Pham, F. van Mourik, C. Bressler, M. Chergui, J. Am. Chem. Soc. **2007**, 129, 8199.
[9] C. Bressler, C. Milne, V.-T. Pham, A. ElNahhas, R. M. van der Veen, W. Gawelda, S. Johnson, P. Beaud, D. Grolimund, M. Kaiser, C. N. Borca, G. Ingold, R. Abela, M. Chergui, Science **2009**, 323, 489.
[10] A. Cannizzo, C. Milne, C. Consani, W. Gawelda, C. Bressler, F. van Mourik, M. Chergui, Coordination Chemistry Reviews **2010**, 254, 2677.
[11] W. Zhang, R. Alonso-Mori, U. Bergmann, C. Bressler, M. Chollet, A. Galler, W. Gawelda, R. G. Hadt, R. W. Hartsock, T. Kroll, K. S. Kæ; K. Kubiček, H. T. Lemke, H. W. Liang, D. A. Meyer, M. M. Nielsen, C. Purser, J. S. Robinson, E. I. Solomon, Z. Sun, D. Sokaras, T. B. van Driel, G. Vankó, T.-C. Weng, D. Zhu, K. J. Gaffney, Nature **2014**, 509, 345.
[12] G. Auböck, M. Chergui, Nat. Chem. **2015**, 7, 629.
[13] H. T. Lemke, K. S. K. R. Hartsock, T. B. van Driel, M. Chollet, J. M. Glownia, S. Song, D. Zhu, E. Pace, S. F. Matar, M. M. Nielsen, M. Benfatto, K. J. Gaffney, E. Collet, M. Cammarata, Nat. Commun. **2017**, 8, 15342.
[14] C. de Graaf, C. Sousa, Chem. Eur. J. **2010**, 16, 4550.
[15] A. Domingo, C. Sousa, C. de Graaf, Dalton Trans. **2014**, 43, 17838.
[16] C. Sousa, C. de Graaf, A. Rudavskyi, R. Broer, J. Tatchen, M. Etinski, C. M. Marian, Chemistry – A European Journal **2013**, 19, 17541.
[17] C. Sousa, M. Llunell, A. Domingo, C. de Graaf, Phys. Chem. Chem. Phys. **2018**, 20, 2351.
[18] L. C. Liu, Photoinduced Spin Crossover in Iron(II) Systems, pages 105–161, Springer International Publishing **2020**.
[19] M. Alías-Rodríguez, M. Huix-Rotllant, C. de Graaf, Faraday Discuss. **2022**, 237, 93.
[20] G. Chastanet, M. Lorenc, R. Bertoni, C. Desplanches, Comptes Rendus Chimie **2018**, 21, 1075.
[21] T. J. Penfold, E. Gindensperger, C. Daniel, C. M. Marian, Chemical Reviews **2018**, 118, 6975.
[22] L. M. Lawson Daku, A. Vargas, A. Hauser, A. Fouqueau, M. E. Casida, ChemPhysChem **2005**, 6, 1393.
[23] J. K. McCusker, K. N. Walda, R. C. Dunn, J. D. Simon, D. Magde, D. N. Hendrickson, J. Am. Chem. Soc. **1992**, 114, 6919.
[24] C. Consani, M. Prémont-Schwarz, A. ElNahhas, C. Bressler, F. van Mourik, A. Cannizzo, M. Chergui, Angew. Chem. **2009**, 121, 7320.
[25] R. M. Berger, D. R. McMillin, Inorganica Chim. Acta **1990**, 177, 65.
[26] P. S. Braterman, J.-I. Song, R. D. Peacock, Inorg. Chem. **1992**, 31, 555.
[27] J. K. McCusker, K. N. Walda, R. C. Dunn, J. D. Simon, D. Magde, D. N. Hendrickson, J. Am. Chem. Soc. **1993**, 115, 298.
[28] A. Moguilevski, M. Wilke, G. Grell, , S. I. Bokarev, S. G. Aziz, N. Engel, A. A. Raheem, O. Kehn, I. Y. Kiyan, E. F. Aziz, Chem. Phys. Chem. **2017**, 18, 465.
[29] M. Pápai, G. Vankó, T. Rozgony, T. J. Penfold, J. Phys. Chem. Lett. **2016**, 7, 2009.
[30] M. Pápai, Inorg. Chem. **2021**, 60, 13950.
[31] M. Pápai, J. Chem. Theory Comput. **2022**, 18, 1329.

ENTRY FOR THE TABLE OF CONTENTS

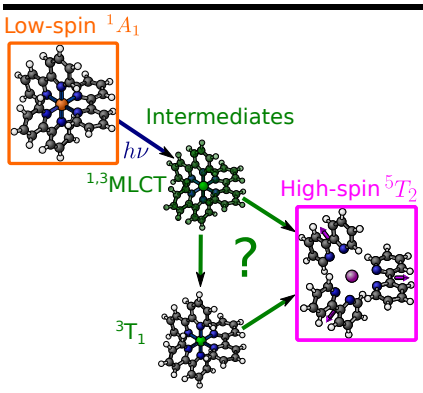

Light-induced spin crossover of $[Fe^{II}(2,2'-bipyridine)_3]^{2+}$ is a reaction converting iron from a low-spin to a high-spin state upon irradiation. Employing wavepacket dynamics, we determine the intermediates responsible for this ultrafast reaction.